Impact of nucleon transfer channels on complete fusion in the ^{6,7}Li $+$ ^{58}Ni reactions near the Coulomb barrier

Vandana Tripathi [ORCID],[*] K. W. Kemper [ORCID], L. T. Baby, P. C. Bender,[†] and S. L. Tabor [ORCID]
Department of Physics, Florida State University, Tallahassee, Florida 32306, USA

N. Keeley[‡]
National Centre for Nuclear Research, ul. Andrzeja Sołtana 7, 05-400 Otwock, Poland

Reactions involving weakly bound nuclei, both stable and radioactive, especially at energies near the Coulomb barrier remain at the forefront as topics to be understood, both experimentally and theoretically. Of special interest is the interplay between complete fusion, breakup, and direct reactions for these cases and the complete understanding of their influence on fusion, which arises because of the bottleneck in experimentally identifying complete fusion events. In this work we address this issue by measuring individual residue cross sections in the interaction of ^{6,7}Li on a thin ^{58}Ni target at energies around the barrier. Comparison with statistical model calculations and coupled reaction calculations allowed us to delineate the reaction products into those arising from complete fusion and those from direct transfer. At energies below the barrier where cross section enhancement is found to occur, the contribution of transfer channels to the total cross section is found to be large and had to be accounted for before assessing the enhancement above the one-dimensional barrier penetration predictions.

I. INTRODUCTION

Fusion of two heavy ions ($A > 4$) is a complex phenomenon which continues to intrigue us, owing to its importance in a wide variety of stellar burning scenarios [1]. At energies above the Coulomb barrier the cross sections are better understood and have a simple linear relationship with energy. However, when the incident energy is lower than or close to the Coulomb barrier, fusion occurs due to quantum tunneling and the cross sections become difficult to predict [2–4]. At these energies one finds an intense interplay between the structure of the colliding nuclei and the reaction mechanism that ensues. The quantum tunneling probability, and hence the fusion cross section, is sensitive to the internal structure of the target and projectile and is found to be enhanced compared to the scenario where the projectile and target are structureless or point particles [5]. Quantum tunneling under the influence of dissipative environments plays an important role and is a fundamental problem in many fields of physics and chemistry. Heavy-ion sub-barrier fusion reactions thus are good examples of environment-assisted tunneling phenomena. For example, the fusion probability of the ^{16}O projectile with ^{144}Sm and ^{154}Sm targets [6] differs substantially at energies below the Coulomb barrier, with the heavier deformed

target showing a larger enhancement of its cross section at the same energy relative to the barrier with similar observations for the ^{40}Ca $+$ ^{90,96}Zr [7,8] systems, where the possibility of neutron transfer for the more neutron-rich target enhances the fusion probability. In the framework of coupled channels (CC) calculations, the coupling of the relative motion of the two colliding nuclei to their internal degrees of freedom (like the rotational states in ^{154}Sm or neutron transfer for ^{96}Zr) assists the quantum tunneling [9–12]. In this regard, the influence of nucleon transfer is the least understood process [13] due to both the inability to include accurately transfer couplings in CC calculations and also missing experimental information on transfer probabilities.

In cases where one of the colliding nuclei is weakly bound, stable, or radioactive, new modes of excitation open up affecting the fusion process [14]. The continuum, being close to the ground state, can be easily excited; additionally the loosely bound valence nucleons enhance the probability of transfer. These dynamic effects along with the likely larger radii of these nuclei are bound to enhance the fusion probability at energies around the barrier. However, the small binding energy of weakly bound nuclei also increases the probability of breakup, the effect of which on the fusion probability is currently under debate [15,16]. Certain models predict the fusion cross section to be enhanced, when compared to the fusion induced by strongly bound nuclei. On the other hand, some models suggest the hindrance of complete fusion, due to the loss of incident flux in this channel, caused by the breakup [17]. This has led to the continued interest in understanding the fusion of stable weakly bound nuclei, like ^{6,7}Li

[*]vtripath@fsu.edu
[†]Present address: Department of Physics, University of Massachusetts Lowell, Lowell, Massachusetts 01854, USA.
[‡]nicholas.keeley@ncbj.gov.pl

and ^{9}Be which have small separation energies ranging from 1.48 to 2.45 MeV. For these cases the influence of transfer and breakup channels on the fusion process can be explored, extensively aided by the high intensity of these stable beams. The main observations under discussion are whether the fusion involving weakly bound nuclei is enhanced, hindered, or not affected at above- and below-barrier energies owing to the strong breakup channel [18–20]. Also in question is the relative contribution of direct reactions like transfer as compared to the fusion channel to the total reaction cross section. As emphasized by the vanishing of the usual threshold anomaly in scattering involving weakly bound nuclei, the breakup cross sections are large even at sub-barrier energies [21]. This points to the fact that, unlike tightly bound nuclei, fusion is not the largest component of the total reaction cross section of weakly bound nuclei; other direct reaction channels may be equally important. Here again, the contribution of transfer channels to the total reaction cross section remains elusive, with not many experiments addressing this issue. A comprehensive discussion of the various aspects of the fusion process involving weakly bound nuclei, theoretical predictions, and experimental data can be found in Ref. [22]

Before proceeding, we will look at the possible outcomes when a typical weakly bound projectile like ^{6}Li collides with a target of mass (A) around 60. The low threshold against breakup, in this particular case only 1.48 MeV, can lead to reaction products where part of the fragment is captured by the target, leading to incomplete fusion (ICF), noncapture breakup (NCBU), or elastic breakup where both of the breakup fragments are observed. For complete fusion (CF) to occur, the projectile and target must fuse together fully before cooling off by emitting particles and γ rays. Also possible is complete fusion following breakup, whereby both fragments are eventually absorbed by the target, which is indistinguishable from the direct complete fusion (CF). The other possibilities are few nucleon transfer (TR) and inelastic reactions. The sum of complete and incomplete fusion is generally referred to as total fusion (TF), while the sum of all the above will be the total reaction cross section. Figure 1 shows the various possibilities schematically. What is immediately obvious is the possibility that transfer (TR) can yield residues similar to ICF. This leads to one of the bottlenecks that has been encountered in analyzing reactions involving weakly bound light projectiles, namely, the difficulty in experimentally disentangling the various reaction products which, makes systematic analysis and comparison with theory difficult.

In this work we report on the measurement of residue cross sections for ^{6,7}Li $+ ^{58}$Ni reactions at incident energies between 10 and 22 MeV in the laboratory frame, covering the region around the Coulomb barrier ($V_B \approx 12$ MeV) for the two systems. The likely origin of the heavy residues is the cooling of the compound nucleus by evaporating particles (i.e., evaporation residues henceforth called ERs). Their cross section thus contributes to complete fusion. However, due to the low breakup threshold of ^{6}Li (≈ 1.5 MeV) and ^{7}Li (≈ 2.5 MeV) one can expect to see significant yields from ICF and transfer, the end products of which will be similar to ERs from CF. There is limited data on fusion cross sections of weakly bound stable beams on medium-mass targets. One of
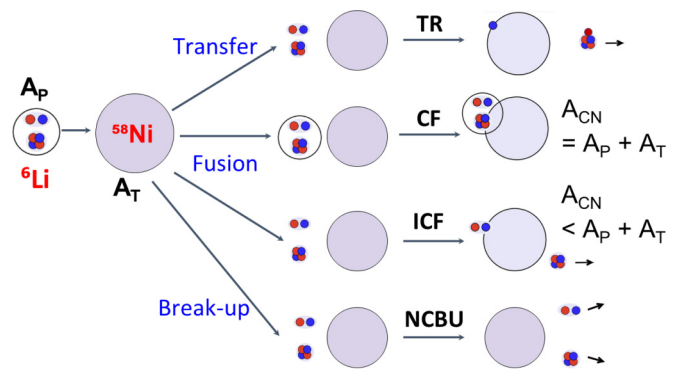

FIG. 1. A schematic showing the possible outcomes when a loosely bound projectile like ^{6}Li interacts with a target (medium mass) at energies around the Coulomb barrier. Fission is not considered an option as the CN is low mass. TR, CF, ICF, and NCBU stand for transfer, complete fusion, incomplete fusion, and noncapture breakup respectively, as discussed in the text.

the reasons for the paucity of such systematic data is the difficulty in measuring the residues directly, as the recoils have very low recoil energy in this asymmetric combination, especially at below-barrier energies. In spite of that fusion cross sections for the ^{6,7}Li $+ ^{64}$Zn systems have been measured by detecting the ERs [15,23]. Recently Aguilera *et al.* [24] measured the fusion cross section for the ^{6}Li $+ ^{58}$Ni system at mostly below-barrier energies by measuring the evaporated protons. Detection of γ rays and x rays has been employed before to obtain fusion cross sections in the ^{6,7}Li $+ ^{59}$Co [25], ^{6}Li $+ ^{64}$Ni [26], and ^{6,7}Li $+ ^{64}$Ni [27] systems. In the present experiment we have extended the measurement to lower energies, reaching about $0.75 V_B$ for the ^{6,7}Li $+ ^{58}$Ni systems, enabled by using the prompt γ-ray yields to extract the fusion cross sections.

II. EXPERIMENTAL DETAILS

The experiment to measure residue cross sections for the ^{6,7}Li $+ ^{58}$Ni systems at energies around the Coulomb barrier was carried out at the John D. Fox Superconducting Accelerator Laboratory at Florida State University (FSU). Beams of ^{6,7}Li^{3+} were provided by the 9 MV tandem accelerator at FSU in the energy range 10 to 22 MeV. The average beam current was around 2 p nA, measured in a Faraday cup at the end of the beam line. The target used was a thin 150 μg/cm^2 self-supporting foil of isotopically enriched ^{58}Ni mounted on a Ta frame. A collimator was used upstream of the target to guide the beam. The characteristic γ rays from the evaporation residues were detected in two Compton-suppressed high-purity germanium detectors of clover type placed at 90° with respect to the target. In this configuration, the Doppler shift, if any, can be avoided and the spectra are easy to analyze. A typical spectrum collected for ^{6}Li on ^{58}Ni at 20.5 MeV incident energy is shown in Fig. 2, where the characteristic γ rays from several of the evaporation residues can be easily identified. The clover detectors were energy and efficiency calibrated using standard ^{60}Co and ^{152}Eu sources at the target position.

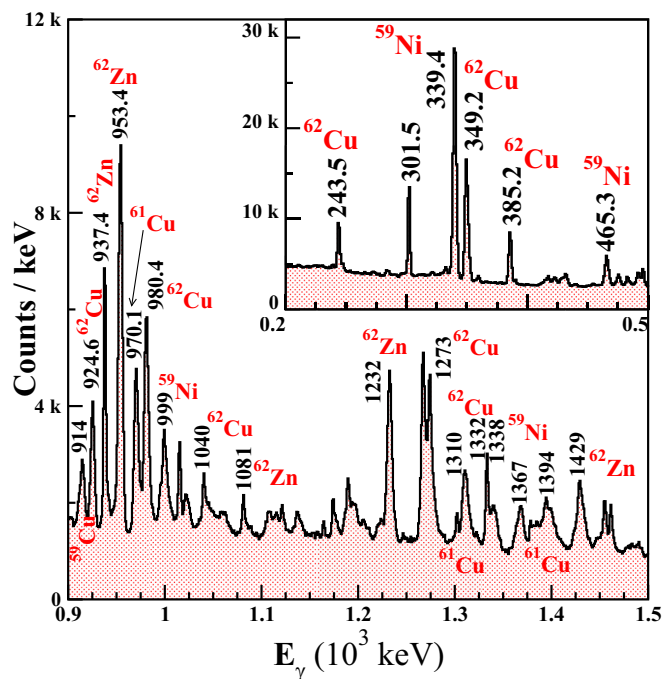FIG. 2. A typical γ spectrum as recorded by the clover detectors at an incident ^{6}Li energy of 20.5 MeV. Characteristic γ rays from the dominant residues are clearly identified. The yields of the γ transitions are proportional to the production cross sections and were used to extract the cross section as a function of energy after correcting for the efficiency of the detectors.

The elastically scattered ^{6,7}Li particles were detected by a Si monitor detector covering a solid angle of 0.025 msr placed at 25° to the beam direction to determine the absolute cross section, since at this angle the elastic scattering follows the Rutherford formula. The choice of a thin target, apart from better incident energy definition, was made to avoid the decay of the stopped residues that would occur in a thick or backed target. The β unstable residues formed in the reactions have lifetimes ranging from minutes to hours and therefore decayed in the Faraday cup about 1 m downstream of the target, out of the sight of the γ detectors. Thus, no γ decays from the β decay of residues were observed. Since the recoil energy of the reaction products even at the highest energy is less than 2 MeV, the recoils would have a velocity of less than 0.25 cm/ns and all the low lying fast electromagnetic transitions would still occur at or infinitely close to the target position so that the determination of the efficiency of the γ detectors by the sources at the target position is valid.

The data were collected in "singles" mode whereby no electronic gating conditions were applied. The signal from the monitor detector was downscaled for data collection to avoid increasing the dead time. A pulser set at a frequency of 10 Hz was fed to the test input of the γ detector and also read in a scaler to estimate the dead time. The beam current was adjusted so as to keep a uniform dead time during the whole run. The excitation function for both systems was measured in steps of around 1 MeV starting from the lowest energy moving upwards to avoid the buildup of any activity in the target.

As mentioned before, the asymmetric nature of the reaction imparts very little kinetic energy to the recoiling residues, making their direct detection nearly impossible. Also, the residues being light, are stable towards α emission, ruling out the other successful method used with heavier targets, namely measuring α decay. For such cases, detection of in-beam characteristic γ rays ensuing from the residues (and in some cases delayed γ rays) is the most viable way of extracting fusion cross sections. Though the γ ray technique circumvents the issue of low recoil energy, it works well only when the low lying level structure of the residues is well known, which is true in this particular case.

III. RESULTS

The fusion excitation functions for both systems, ^{6,7}Li $+$ ^{58}Ni, were measured covering the energy range 10 to 22 MeV in the laboratory frame. The fusion cross sections at each energy were obtained by adding the various residue cross sections. The heavy residues have been loosely called fusion products here; however, they may have contributions from other reaction processes, as will be discussed later. All the residues that are expected to be produced have been studied by heavy ion reactions before, hence their decay structure is well known. Also, the absence of long lived isomers makes the extraction of cross sections possible and reliable. The in-beam γ transitions that feed the ground state of the different residues were collected to calculate the production cross section for that residue. The use of a thin target and measuring the excitation functions in increasing order of energy ensured that the in-beam data were not affected by the decay of the residues, as was seen in the ^{6,7}Li $+$ ^{59}Co [14] measurement. The efficiency corrected yields of the γ rays were normalized by the counts in the monitor detector measuring pure Rutherford scattering. The measured residue cross sections as a function of the incident laboratory energy are shown in Fig. 3 (bottom panel) which also shows the results of statistical model calculations using PACE4 (top panel) for energies above the Coulomb barrier [28]. Default parameters were used for PACE4, with little sensitivity to the choice of level density parameter seen for the small cross sections. The comparison with PACE4 predictions here is mainly to judge the relative importance of the different evaporation channels and not for their absolute values.

A close look at the residue cross sections in the ^{6}Li $+$ ^{58}Ni reaction shown in Fig. 3(a) reveals discrepancies in the production of ^{59}Ni and ^{59}Cu residues in comparison to a pure fusion evaporation scenario (PACE4 calculations), where they would be the αp and αn evaporation channels. ^{59}Ni is the biggest cross section at all energies, while the ^{59}Cu excitation function falls slower than that predicted by PACE4, indicating additional contributions at below-barrier energies. The alternate ways which can lead to the same residues are n-stripping or p-stripping reactions. The Q_{gg} values for n stripping and d stripping are positive (3.325 and 9.779 MeV, respectively) while for p stripping Q_{gg} is -1.015 MeV. As is known, transfer reactions are driven by optimum Q-value matching conditions, which means that classically the entrance and exit trajectories must match smoothly. The optimum Q value for transfer, Q_{opt}, is approximately zero for n stripping and
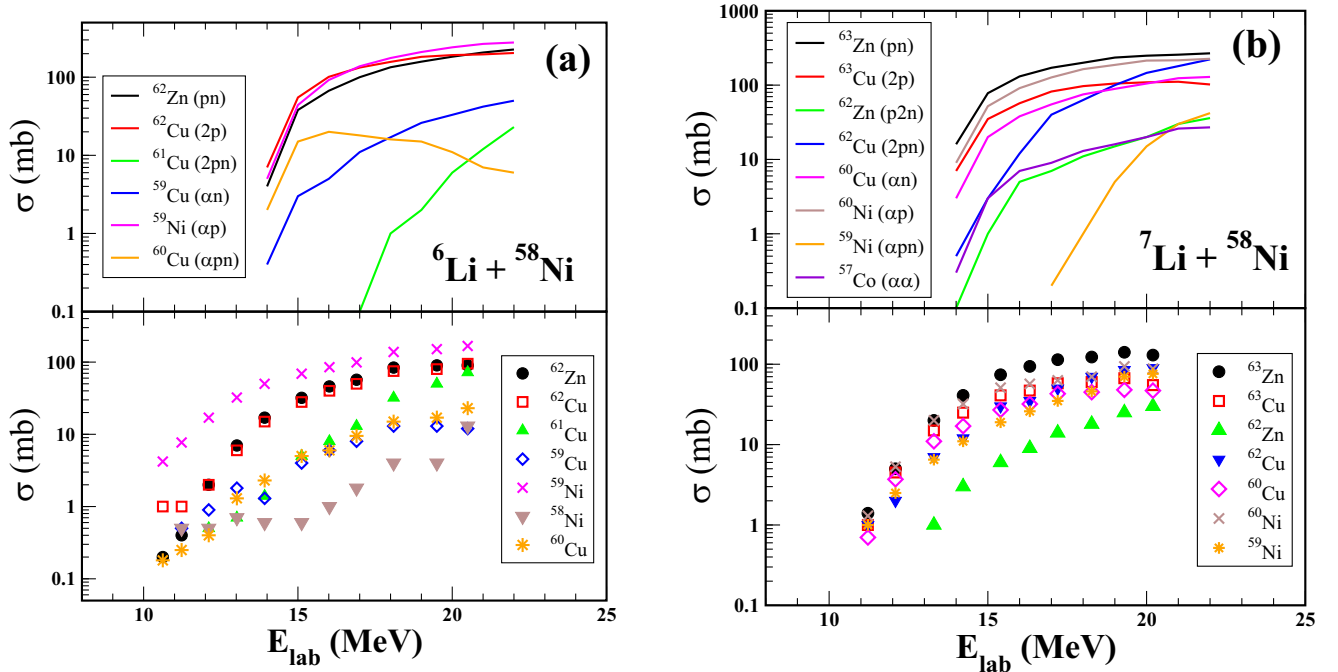
FIG. 3. Bottom panel: The measured residue cross sections for the two systems [(a) ^{6}Li + ^{58}Ni and (b) ^{7}Li + ^{58}Ni] as a function of the incident beam energy. Top panel: The corresponding predictions of the statistical model code PACE4.

$-0.31E_{cm}$ for p and d stripping. This implies that the n and d stripping will preferentially populate excited states in the residual nuclei and not the ground state. In the case of d stripping populating ^{60}Cu, the excitation energy E^* ($= Q_{opt} + Q_{gg}$) will range between 12.7 and 15.5 MeV, which is well above the proton and neutron separation energies (S_p of 4.5 MeV and S_n of 10.06 MeV). So it is most likely that d transfer will also populate states in ^{59}Ni and ^{59}Cu after proton and neutron evaporation.

For the ^{7}Li + ^{58}Ni reaction, the only evaporation residue that deviates from the PACE4 predictions as shown in Fig. 3(b) is ^{59}Ni. The αpn cross section is expected to fall off sharply approaching the barrier; however, the experimental cross section does not. In this case, too, the mode of production of ^{59}Ni could be n stripping and also t transfer. The Q_{gg} for t transfer is +14.239 MeV, implying again that a highly excited ^{61}Cu will be produced. At that excitation energy ^{61}Cu is expected to cool down by emitting a proton and neutron leading again to ^{59}Ni. Thus, in both these reactions, we see the likely presence of transfer products. In principle the same residue will be produced as a result of d or t fusion and subsequent evaporation. However, the fact that these residues are more pronounced at below barrier energies suggests that their production is not governed by the Coulomb barrier, and hence is more likely to be from transfer.

The total fusion cross section is obtained by the addition of the different residue components. There are two things that need to be kept in mind in this regard: first, what fraction of the total fusion cross section do the measured residues represent, and second, as always with any absolute cross section measurement, whether the absolute normalization is correct or not. As per the statistical model calculations, the measured residues constitute more than 95% of the fusion cross section

for both reactions, so underestimation is not a worry here. However, as mentioned before, the fusion cross section might be overestimated due to contributions from transfer which cannot be separated. As for the absolute normalization, the fact that we had one collimator upstream of the target and only one monitor and the use of a thin target leaves room for error in the absolute normalization. In recent studies of the breakup of ^{6,7}Li on light targets like ^{58}Ni and ^{64}Zn, direct breakup has been found to be negligible [29] and, hence, suppression of the complete fusion reaction is not expected at energies above the Coulomb barrier. A similar inference was reached by Diaz-Torres *et al.* [30] based on continuum discretized coupled channel calculations for ^{6,7}Li + ^{59}Co systems, i.e., breakup hardly affects the total fusion at energies well above the barrier.

As we do not expect fusion suppression at above-barrier energies, the total residue cross sections at the two highest energies (assumed to be complete fusion) was renormalized to the theoretical estimate at those energies taken from a coupled channel calculation using the code CCFULL [31] without any couplings. Without including any coupling, the CCFULL calculation is just the simple one-dimensional barrier penetration model (1D-BPM) for fusion. Otherwise, CCFULL is a full quantum mechanical solution of the coupled equations where the relative motion between the target and projectile is coupled to the intrinsic degrees of freedom. The coupled equations are solved under the ingoing-wave boundary condition [32], which provides a more realistic framework for describing fusion reactions. Within the coupled-channel formalism one determines the total reaction cross section and the total cross section in the excited channels. This difference is equal to the ingoing flux at the barrier radius and is equated with the fusion cross section. The critical input in this code is the bare
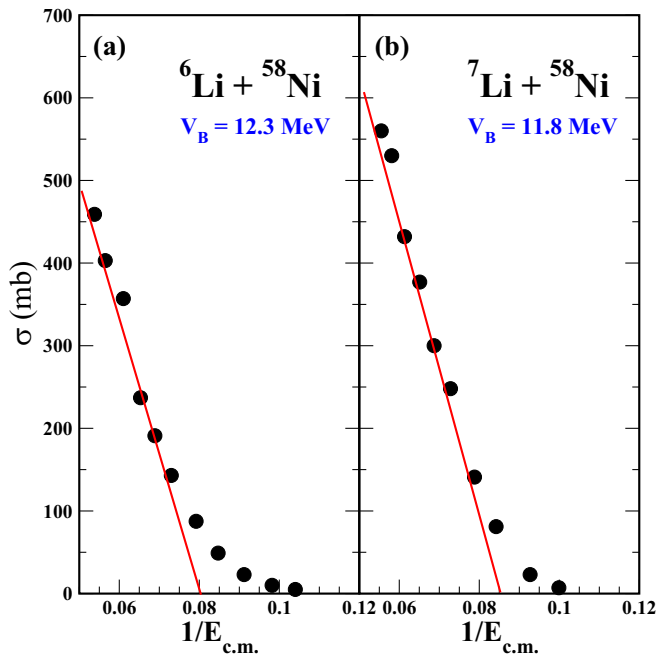
FIG. 4. The measured fusion cross section plotted as a function of the inverse of the incident energy in the center-of-mass frame. The linear dependence of the fusion cross section at energies above the barrier allows us to extract the Coulomb barrier as the intercept on the x axis of the straight line through the above-barrier data points.

potential to be used. The parameter-free Sao Paulo potential (SPP) [33] was used in the calculations as it has been greatly successful in explaining features of the reaction mechanisms involving both strongly bound and weakly bound projectiles like ^{16,18}O, ^{6,7}Li and ^{9}Be. This potential is based on a double folding potential and on the Pauli nonlocality involving exchange of nucleons between projectile and target. As input to the CCFULL code, an equivalent local Woods-Saxon (WS) potential was extracted, having similar strengths in the surface region as those of the realistic SPP. The WS parameters used were $V_0 = 75.0$ MeV, $r_0 = 1.05$ fm, and $a = 0.72$ fm for the ^{6}Li induced reaction and $V_0 = 99.0$ MeV, $r_0 = 1.06$ fm, and $a = 0.72$ fm for the ^{7}Li beam. These parameters yielded a Coulomb barrier (V_B) of 12.34 and 11.83 MeV for the ^{6}Li and ^{7}Li induced reactions, respectively, in complete agreement with the empirical values obtained by fitting the above barrier cross sections as shown in Fig. 4.

IV. DISCUSSION

The total measured residue cross sections for both ^{6,7}Li + ^{58}Ni reactions are shown in Fig. 5 by the black symbols. When compared to the predictions of CCFULL in the no coupling limit (dashed green line in Fig. 5), the total residue cross section is clearly enhanced at below-barrier energies with more enhancement for the ^{6}Li case. Including coupling to the low lying collective states in the target (both the quadrupole, 2^+, and octupole, 3^-, vibrations) does little in terms of producing enhancement as can be seen by the solid lines in both panels of Fig. 5. The reason for this is
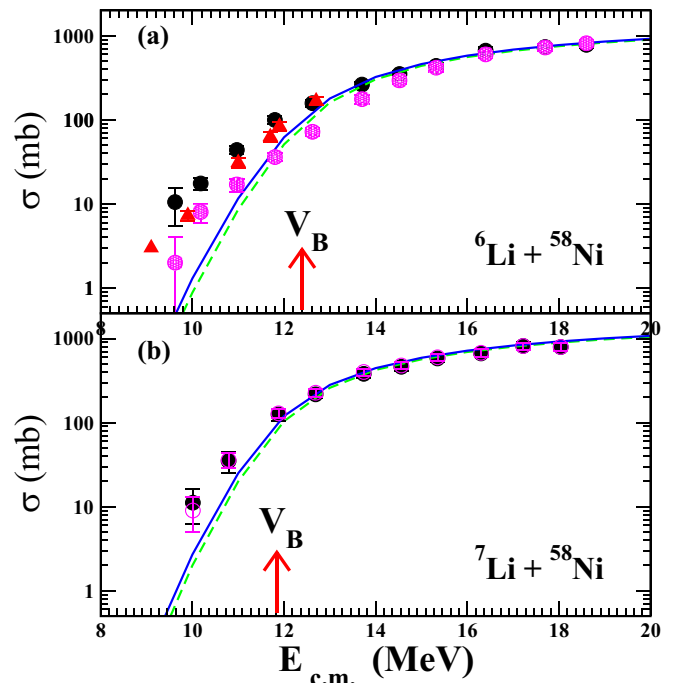

FIG. 5. Total residue cross sections for the two systems as a function of the center-of-mass energy along with coupled-channels calculations performed using the code CCFULL. Black circles represent the sum of all the residues that were measured and thus the sum of fusion and transfer cross sections. The magenta symbols on the other hand represent the estimated complete fusion cross sections. Here the cross sections for the production of ^{59}Ni and ^{59}Cu have been replaced by the PACE4 estimates. The dashed lines represent coupled channels calculations with no coupling included and, hence, present the predicted cross section in a one-dimensional barrier penetration model. The solid lines include coupling to inelastic excitations of the target. Additionally, we also show as red triangles the measured fusion cross section for ^{6}Li + ^{58}Ni from Ref. [24].

the low value of $Z_P Z_T$ in this case. As discussed before, there is an enhancement of certain residues, namely ^{59}Ni (for both ^{6,7}Li) and ^{59}Cu for ^{6}Li, as compared to what is expected for compound nucleus evaporation, which can be attributed to nucleon transfer in both cases.

In order to verify that the residues ^{59}Ni and ^{59}Cu are the products of transfer reactions, coupled reaction channels (CRC) calculations were performed using the code FRESCO [34] to model the formation of ^{59}Ni and ^{59}Cu via single-nucleon stripping reactions for both ^{6}Li and ^{7}Li projectiles incident on ^{58}Ni. The calculations included couplings to the 1.454-MeV 2_1^+ level of ^{58}Ni for both projectiles and ground state reorientation and excitation of the 0.478-MeV $1/2^-$ level of ^{7}Li in addition to the stripping. For ^{6}Li, only stripping leaving the final ^{5}Li (n stripping) and ^{5}He (p stripping) in their $3/2^-$ ground states was considered since the $1/2^-$ levels are very broad. For ^{7}Li, stripping leaving the final ^{6}Li (n stripping) in both its 1^+ ground and 2.18-MeV 3^+ resonant states was included, as was coupling between these two levels. Stripping leaving the final ^{6}He (p stripping) in its 0^+ ground state only was considered since the relatively large negative

Q value for this reaction (-6.56 MeV) leads to a negligible contribution from stripping to the 1.80-MeV 2^+ resonance. The ^{58}Ni 2^+_1 level was treated as a single-phonon collective vibrational state with the $B(E2)$ value taken from Raman *et al.* [35] and the corresponding nuclear deformation length, $\delta_2 = 0.78$ fm, extracted from the $B(E2)$ using the collective model and assuming a charge radius of $1.3 \times 58^{1/3}$ fm. The $3/2^-$ ground state and $1/2^-$ level of ^{7}Li were treated as members of a $K = 1/2$ rotational band with the $B(E2)$ taken from Ref. [36] and the nuclear deformation length, $\delta_2 = 2.0$ fm, from Ref. [37]. The 1^+ ground state and 3^+ resonance of ^{6}Li were assumed to be members of a $K = 1$ rotational band with the exception that reorientation of the 1^+ ground state was omitted due to the very small quadrupole moment of this level. The $B(E2)$ was taken from Ref. [38] and the nuclear deformation length $\delta_2 = 1.9$ fm from Ref. [39].

All optical model potentials consisted of a double-folded real part and a Woods-Saxon squared imaginary part. The parameters of the Woods-Saxon squared potentials were $W = 50$ MeV, $R = 1.0 \times (A_p^{1/3} + A_t^{1/3})$ fm, $a_W = 0.3$ fm, effectively reproducing the incoming-wave boundary condition [40]. The double-folded potentials were calculated with the code DFPOT [41] and the M3Y nucleon-nucleon effective interaction [42]. The ^{6}Li and ^{7}Li densities were taken from Refs. [43] and [44], respectively, the charge density of Ref. [43] being converted to the nuclear matter density by unfolding the proton charge density and assuming that $\rho_{\text{Nuc}} = (1 + N/Z)\rho_p$. The ^{6}He matter density was taken from Tanihata *et al.* [45] and the ^{5}He and ^{5}Li densities from Refs. [46] and [47], respectively. For ^{58}Ni, ^{59}Ni, and ^{59}Cu the RIPL-3 HFB14 densities [48] were used. The spectroscopic amplitudes for the $\langle ^6$Li $\mid ^5$Li $+ n\rangle$, $\langle ^6$Li $\mid ^5$He $+ p\rangle$, $\langle ^7$Li $\mid ^6$Li $+ n\rangle$, and $\langle ^7$Li $\mid ^6$He $+ p\rangle$ overlaps were taken from Cohen and Kurath [49]. The spectroscopic factors for the $\langle ^{59}$Ni $\mid ^{58}$Ni $+ n\rangle$ overlaps were taken from Lee *et al.* [50]. However, due to the large number involved, for a given spin-parity the set of n actual levels was in each case replaced by a single level with a summed spectroscopic factor C^2S_{lsj} and a weighted mean excitation energy E_{ex} obtained as follows:

$$C^2S_{lsj} = \sum_{i=1}^{n} C^2S_{lsj}^i,$$

$$E_{\text{ex}} = \frac{\sum_{i=1}^{n} C^2S_{lsj}^i E_{\text{ex}}^i}{\sum_{i=1}^{n} C^2S_{lsj}^i}. \tag{1}$$

The $3/2^-$ ground state of ^{59}Ni was excluded from this procedure since direct population of the ground state cannot be measured using the characteristic γ-ray technique employed. It was therefore included in the CRC calculations as a separate single level. A similar summation was not necessary for the $\langle ^{59}$Cu $\mid ^{58}$Ni $+ p\rangle$ overlaps since the number of levels concerned was much smaller, and the required spectroscopic factors were taken directly from Bindal *et al.* [51].

The results are the summed cross sections for populating all levels in ^{59}Ni or ^{59}Cu excluding the ground state to make comparison with the measured cross sections. The results along with the experimental data are shown in Fig. 6. The black solid curves represent the predictions for ^{59}Ni and the
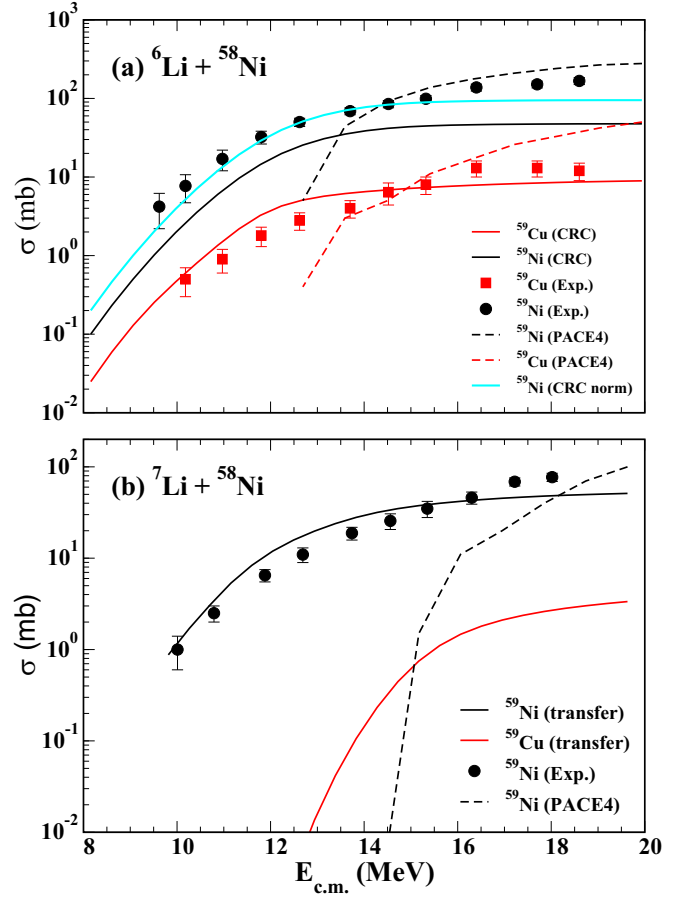

FIG. 6. Measured n-stripping and p-stripping transfer cross sections as compared to CRC using the code FRESCO for the ^{6}Li $+ ^{58}$Ni and ^{7}Li $+ ^{58}$Ni systems. See text for further details.

red for ^{59}Cu, as detailed above. For both ^{6,7}Li induced reactions, the production of ^{59}Ni as a result of $1n$ neutron transfer follows very nicely the trend of the measured cross section, especially at the lower energies. For $E_{\text{cm}} > \approx 15$ MeV, the contribution from fusion evaporation kicks in as indicated by the PACE4 predictions shown by the dashed curves in Fig. 6. Overall the results are very good for both ^{6,7}Li although there is a definite overprediction of the ^{59}Ni cross section at the lower energies in the case of the ^{6}Li induced reactions. The calculations also confirm why we do not see any proton stripping (^{59}Cu) for ^{7}Li as the predicted cross sections are too small, even at the highest energies.

Based on the CRC calculations (Fig. 6), it can be safely said that the mechanism of production of ^{59}Ni and ^{59}Cu is a combination of fusion evaporation and transfer, with transfer being the dominant process at energies below the barrier. With this information, we have estimated the complete fusion cross section for the ^{6,7}Li $+ ^{58}$Ni reactions by replacing the measured cross sections for ^{59}Ni and ^{59}Cu with the PACE4 estimates, and these results are shown by the magenta symbols in Fig. 5. Now there seems to be reasonable agreement between the data and the CCFULL calculations including the inelastic coupling to target states. The slight overprediction at the lowest energies could be a signal of coupling to other
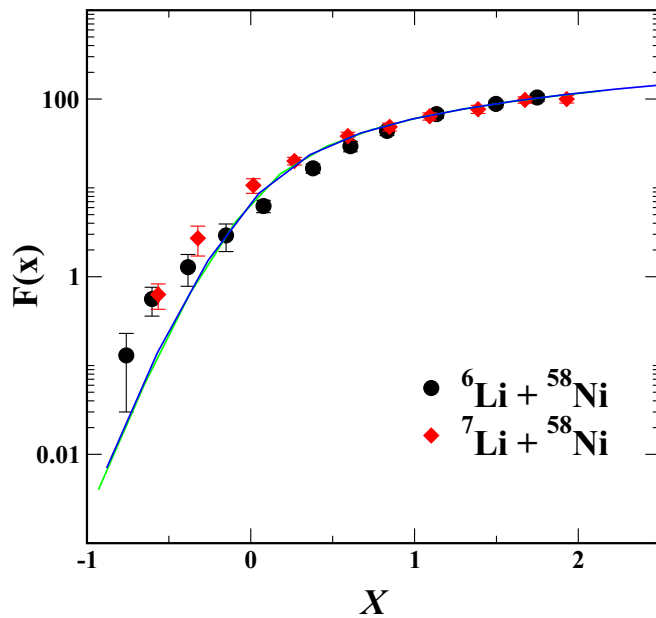
FIG. 7. Comparison of ^{6,7}Li + ^{58}Ni data in the reduced scale so as to cancel out the geometric effects. The reduced energy is given by the dimensionless quantity $X = \frac{(E_{cm} - V_b)}{\hbar \omega}$ and the reduced fusion cross section is given by the function $F(x) = \frac{2E_{cm} \sigma(E_{cm})}{\hbar \omega R_b^2}$. The barrier parameters were taken from the CCFULL calculations discussed in the text. The predictions for the 1D-BPM are also shown by the solid lines for each system though they overlap completely as expected.

degrees of freedom which is likely to be transfer or breakup in this case. In the absence of reliable form factors we did not attempt to include transfer coupling in the CCFULL calculations. In Fig. 5 we have also displayed by red triangles the fusion cross section for the ^{6}Li + ^{58}Ni system obtained by detecting the protons from Ref. [24]. There is reasonable agreement between the two measurements; the differences could arise from the fact that the proton measurement was limited to below-barrier energies, causing potential normalization issues, and also a natural Ni target was employed in that measurement.

The modified cross sections represented by the magenta symbols for ^{6,7}Li fusion (Fig. 5) are now displayed in Fig. 7 using the reduced variables from Ref. [33] which take into consideration static and dynamic effects. As can be seen, the two excitation function agree quite well over the entire energy range, again, implying that the special structure of the projectile is playing a small role in the fusion process for these reactions. The reduced cross sections for both the systems also follow closely the predictions of the 1D-BPM until the very lowest energies, where some departure is seen. This could be indicative of the need to include transfer or breakup effects in the calculations as elucidated in the calculation in Ref. [30].

The conclusion that can be thus drawn is that the weak binding of ^{6,7}Li seems to favor significant transfer cross sections but has a much weaker influence on the fusion cross

section. It is seen here, for reactions of ^{6,7}Li on $A \approx 60$, that a large fraction of the cross sections at below-barrier energies originate from transfer, rather than fusion. This may be true for other cases too, where +Q-value transfer channels are present for example, ^{18}O. This is one of the uncertainties when discussing sub-barrier enhancement if the origin of residues cannot be definitely identified. If the transfer and fusion processes cannot be delineated then it will lead to an erroneous conclusion of large sub-barrier complete fusion enhancement. For the present case it is clear that there is very little sub-barrier enhancement, once the yield of transfer channels is accounted for, and the weak binding of the projectile has little influence on the fusion process.

V. SUMMARY

In beam γ-ray spectroscopy was used to measure residue cross sections for the ^{6,7}Li + ^{58}Ni reactions in the energy range, 10 to 22 MeV covering the region around the Coulomb barrier for the two systems. At each incident energy (10 and 11 data points for ^{6}Li and ^{7}Li, respectively), the characteristic γ rays feeding the ground state of each residue were identified and efficiency corrected yields were used to calculate the production cross sections. Comparing the residue cross section with the estimates from the statistical model code PACE4 revealed an excess for two particular residues, namely ^{59}Ni and ^{59}Cu, at below-barrier energies. These residues have been identified to be formed in the one-neutron stripping and one-proton stripping channels, respectively. This conclusion is corroborated by coupled reaction channels calculations. Including these residues in calculating the fusion cross sections leads to a large enhancement of the cross sections at below-barrier energies which is not explained by coupled channel calculations for complete fusion. Properly taking into account the stripping channels results in complete fusion cross sections consistent with calculations. This highlights that at below-barrier energies transfer cross sections can be large for certain reactions and, if not distinguished from evaporation residues, can lead to erroneous conclusions about sub-barrier enhancement. Another point that is highlighted is that even when transfer cross sections are large they do not always lead to a large enhancement of fusion cross sections at below-barrier energies. Understanding the coupling effects of +Q-value transfer channels will require more targeted experiments and systematic analysis in the future.

[1] V. I. Zagrebaev, V. V. Samarin, and W. Greiner, Phys. Rev. C **75**, 035809 (2007).

[2] M. Beckerman, Phys. Rep. **129**, 145 (1985).

[3] M. Beckerman, Rep. Prog. Phys. **51**, 1047 (1988).

[4] A. B. Balantekin and N. Takigawa, Rev. Mod. Phys. **70**, 77 (1998).

[5] M. Dasgupta, D. J. Hinde, N. Rowley, and A. M. Stefanini, Annu. Rev. Nucl. Part. Sci. **48**, 401 (1998).

[6] J. R. Leigh, M. Dasgupta, D. J. Hinde, J. C. Mein, C. R. Morton, R. C. Lemmon, J. P. Lestone, J. O. Newton, H. Timmers, J. X. Wei, and N. Rowley, Phys. Rev. C **52**, 3151 (1995).

[7] A. M. Stefanini, F. Scarlassara, S. Beghini, G. Montagnoli, R. Silvestri, M. Trotta, B. R. Behera, L. Corradi, E. Fioretto, A. Gadea, Y. W. Wu, S. Szilner, H. Q. Zhang, Z. H. Liu, M. Ruan, F. Yang, and N. Rowley, Phys. Rev. C **73**, 034606 (2006).

[8] H. Timmers, D. Ackermann, S. Beghini, L. Corradi, J. H. He, G. Montagnoli, F. Scarlassara, A. M. Stefanini, and N. Rowley, Nucl. Phys. A **633**, 421 (1998).

[9] H. Esbensen, Nucl. Phys. A **352**, 147 (1981).

[10] C. Dasso, S. Landowne, and A. Winther, Nucl. Phys. A **407**, 221 (1983).

[11] C. Dasso, S. Landowne, and A. Winther, Nucl. Phys. A **432**, 495 (1985).

[12] K. Hagino and N. Takigawa, Prog. Theor. Phys. **128**, 1061 (2012).

[13] V. A. Rachkov, A. V. Karpov, A. S. Denikin, and V. I. Zagrebaev, Phys. Rev. C **90**, 014614 (2014).

[14] C. Beck, Nucl. Phys. A **787**, 251c (2007).

[15] P. Gomes, J. Lubian, and R. Anjos, Nucl. Phys. A **734**, 233 (2004).

[16] P. R. S. Gomes, M. D. Rodríguez, G. V. Martí, I. Padron, L. C. Chamon, J. O. Fernández Niello, O. A. Capurro, A. J. Pacheco, J. E. Testoni, A. Arazi, M. Ramírez, R. M. Anjos, J. Lubian, R. Veiga, R. Liguori Neto, E. Crema, N. Added, C. Tenreiro, and M. S. Hussein, Phys. Rev. C **71**, 034608 (2005).

[17] M. Dasgupta, P. R. S. Gomes, D. J. Hinde, S. B. Moraes, R. M. Anjos, A. C. Berriman, R. D. Butt, N. Carlin, J. Lubian, C. R. Morton, J. O. Newton, and A. Szanto de Toledo, Phys. Rev. C **70**, 024606 (2004).

[18] L. Canto, P. Gomes, R. Donangelo, and M. Hussein, Phys. Rep. **424**, 1 (2006).

[19] N. Keeley, R. Raabe, N. Alamanos, and J. Sida, Prog. Part. Nucl. Phys. **59**, 579 (2007).

[20] N. Keeley, N. Alamanos, K. Kemper, and K. Rusek, Prog. Part. Nucl. Phys. **63**, 396 (2009).

[21] F. Torabi, E. Aguilera, O. Ghodsi, and A. Gómez-Camacho, Nucl. Phys. A **994**, 121661 (2020).

[22] L. Canto, P. Gomes, R. Donangelo, J. Lubian, and M. Hussein, Phys. Rep. **596**, 1 (2015).

[23] I. Padron, P. R. S. Gomes, R. M. Anjos, J. Lubian, C. Muri, J. J. S. Alves, G. V. Martí, M. Ramírez, A. J. Pacheco, O. A. Capurro, J. O. Fernández Niello, J. E. Testoni, D. Abriola, and M. R. Spinella, Phys. Rev. C **66**, 044608 (2002).

[24] E. F. Aguilera, E. Martinez-Quiroz, P. Amador-Valenzuela, D. Lizcano, A. García-Flores, J. J. Kolata, A. Roberts, G. V. Rogachev, G. F. Peaslee, V. Guimarães, F. D. Becchetti, A. Villano, M. Ojaruega, Y. Chen, H. Jiang, M. Febbraro, P. A. DeYoung, and T. L. Belyaeva, Phys. Rev. C **96**, 024616 (2017).

[25] C. Beck, F. A. Souza, N. Rowley, S. J. Sanders, N. Aissaoui, E. E. Alonso, P. Bednarczyk, N. Carlin, S. Courtin,

A. Diaz-Torres, A. Dummer, F. Haas, A. Hachem, K. Hagino, F. Hoellinger, R. V. F. Janssens, N. Kintz, R. Liguori Neto, E. Martin *et al.*, Phys. Rev. C **67**, 054602 (2003).

[26] M. M. Shaikh, S. Roy, S. Rajbanshi, M. K. Pradhan, A. Mukherjee, P. Basu, S. Pal, V. Nanal, R. G. Pillay, and A. Shrivastava, Phys. Rev. C **90**, 024615 (2014).

[27] A. Di Pietro, P. Figuera, E. Strano, M. Fisichella, O. Goryunov, M. Lattuada, C. Maiolino, C. Marchetta, M. Milin, A. Musumarra, V. Ostashko, M. G. Pellegriti, V. Privitera, G. Randisi, L. Romano, D. Santonocito, V. Scuderi, D. Torresi, and M. Zadro, Phys. Rev. C **87**, 064614 (2013).

[28] A. Gavron, Phys. Rev. C **21**, 230 (1980).

[29] S. Kalkal, E. C. Simpson, D. H. Luong, K. J. Cook, M. Dasgupta, D. J. Hinde, I. P. Carter, D. Y. Jeung, G. Mohanto, C. S. Palshetkar, E. Prasad, D. C. Rafferty, C. Simenel, K. Vo-Phuoc, E. Williams, L. R. Gasques, P. R. S. Gomes, and R. Linares, Phys. Rev. C **93**, 044605 (2016).

[30] A. Diaz-Torres, I. J. Thompson, and C. Beck, Phys. Rev. C **68**, 044607 (2003).

[31] K. Hagino, N. Rowley, and A. Kruppa, Comput. Phys. Commun. **123**, 143 (1999).

[32] G. H. Rawitscher, Nucl. Phys. **85**, 337 (1966).

[33] L. F. Canto, P. R. S. Gomes, J. Lubian, L. C. Chamon, and E. Crema, J. Phys. G: Nucl. Part. Phys. **36**, 015109 (2008).

[34] I. J. Thompson, Comput. Phys. Rep. **7**, 167 (1988).

[35] C. N. S. Raman and P. Tikkanen, At. Data Nucl. Data Tables **78**, 1 (2001).

[36] S. Chu, L. Hollberg, J. E. Bjorkholm, A. Cable, and A. Ashkin, Phys. Rev. Lett. **55**, 48 (1985).

[37] W. D. Weintraub, N. Keeley, K. W. Kemper, K. Kravvaris, F. Maréchal, D. Robson, B. T. Roeder, K. Rusek, and A. Volya, Phys. Rev. C **100**, 024604 (2019).

[38] F. Ajzenberg-Selove, Nucl. Phys. A **490**, 1 (1988).

[39] S. K. Pandit, A. Shrivastava, K. Mahata, N. Keeley, V. V. Parkar, P. C. Rout, K. Ramachandran, I. Martel, C. S. Palshetkar, A. Kumar, A. Chatterjee, and S. Kailas, Phys. Rev. C **93**, 061602(R) (2016).

[40] M. J. Rhoades-Brown and P. Braun-Munzinger, Phys. Lett. B **136**, 19 (1984).

[41] J. Cook, Comput. Phys. Commun. **25**, 125 (1982).

[42] G. R. Satchler and W. G. Love, Phys. Rep. **55**, 183 (1979).

[43] L. R. Suelzle, M. R. Yearian, and H. Crannell, Phys. Rev. **162**, 992 (1967).

[44] J. Cook, M. F. Vineyard, K. W. Kemper, and V. Hnizdo, Phys. Rev. C **27**, 1536 (1983).

[45] I. Tanihata, D. Hirata, T. Kobayashi, S. Shimoura, S. Sugimoto, and H. Toki, Phys. Lett. B **289**, 261 (1992).

[46] T. Neff and H. Feldmeier, Nucl. Phys. A **738**, 357 (2004).

[47] M. Tomaselli, P. Egelhof, S. R. Neumaier, M. Mutterer, T. Kühl, A. Dax, F. Schmitt, and S. Fritzsche, Hyperfine Interact. **127**, 95 (2000).

[48] R. Capote, M. Herman, P. Obložinský, P. G. Young, S. Goriely, T. Belgya, A. V. Ignatyuk, A. J. Koning, S. Hilaire, V. A. Plujko, M. Avrigeanu, O. Bersillon, M. B. Chadwick, T. Fukahori, Z. Ge, Y. Han, S. Kailas, J. Kopecky, V. M. Maslov, G. Reffo *et al.*, Nucl. Data Sheets **110**, 3107 (2009).

[49] S. Cohen and D. Kurath, Nucl. Phys. A **101**, 1 (1967).

[50] J. Lee, M. B. Tsang, W. G. Lynch, M. Horoi, and S. C. Su, Phys. Rev. C **79**, 054611 (2009).

[51] P. K. Bindal, D. H. Youngblood, and R. L. Kozub, Phys. Rev. C **14**, 521 (1976).